

# Thin Film Electrochemical Memristive Systems for Bio-Inspired Computation

Victor Erokhin\* and M. P. Fontana

*Department of Physics, University of Parma, Viale Uberti 7 A, 43100 Parma, Italy and IPCF-CNR, Rome 00185, Italy*

We present the basic principles of the organization of organic memristor—the circuit element whose conductivity may vary according to its previous involvement in the current conduction. This property is an analog of the synaptic plasticity in biological systems, responsible for learning and memory. We describe also architecture and properties of adaptive networks based on the organic memristors. Finally, we discuss alternative strategies for the construction of statistical adaptive networks with element sizes in the nm range.

**Keywords:** Organic Memristor, Adaptive Networks, Conducting Polymers.

## CONTENTS

1. Introduction . . . . .	313
2. Memristor . . . . .	315
3. Electrochemical Electronic Elements . . . . .	316
4. Organic Memristor . . . . .	317
5. Auto-Oscillating Memristor . . . . .	323
6. Adaptive Networks . . . . .	325
7. Statistical Networks . . . . .	327
8. Conclusions . . . . .	328
Acknowledgments . . . . .	329
References . . . . .	329

## 1. INTRODUCTION

An essential feature of practically all modern computers is the distinctly separated hardware realization of processor and memory elements. There are several technological reasons for such separation. In fact, processing is performed by semiconductor elements based mainly on MIS active elements, while long-term memory is based on magnetic and/or optical properties of materials. Summarizing, memorized information is a “passive medium” having no influence on the properties of elements from which the processor is fabricated. Therefore, no learning and adaptations can be expected at the hardware level in such systems. The only adaptive systems, capable to vary their properties according changes in their environment, so-called neural networks, are currently realized mainly at the software level. In this case the physical separation of the memory and processor elements are not important. All

adaptations take place as variations of the software parameters. Thus, if we consider a situation in which the new task to be solved is very similar to a previously solved one, but formulated in new terms, unrecognized by the previously used software, the hardware will not be prepared to use the already existing algorithms.

The mentioned example is the illustration of the approach which has been very successful, taking into consideration that the modern civilization cannot be imagined without the revolution in the information technologies, impossible without computers. The strategy was based on the available technological capabilities, but it is absolutely different from the paradigms used by nature for “biocomputers.”

In living beings, the same elements of the nervous system are responsible for both memory and information processing. This coincidence of the “hardware” architecture elements allows learning. In the simplest cases it is so called “Pavlov reflections.” However, it is also learning, because the system (animal) establishes associations of indirect inputs (sound in the Pavlov experiments) with absolutely natural ones (presence of food). Thus, the accumulated experience is not only memorized, but has resulted in the modification of the nervous system (“processor”), that allows in a shorter time to resolve similar problems in the future. Even more impressively, a slow processor (“brain”) is able to resolve the problem of the object recognition much faster and in “noisy” conditions (dark, fog, motion, long distance) much more efficiently with respect to the best modern processors, capable to make arithmetical operations with a much higher speed than the human brain. The main reason of such feature is

REVIEW

\*Author to whom correspondence should be addressed.

that the experience, connected to the object identification, has been not only memorized, but has modified the “processor” features, in such a way that the new information analysis can be performed as the parallel comparison of the new information with features of the analyzed objects that have been already identified as the reference point. Such “processor” modification can be connected to the strengthening or inhibition of synaptic connections (Hebbian or synaptic learning<sup>1,2</sup>) or to modification of the neuron body properties (non-Hebbian learning<sup>3,4</sup>).

Even if there is not, fortunately, an absolutely comprehensive model of the brain and even of other parts of the nervous system, there are several models, describing the most probable learning algorithms.

Several alternative algorithms are under discussion, the most classic one being the synaptic algorithm, inspired by the Hebbian paradigm:<sup>1</sup>

When an axon of cell A is near enough to excite cell B and repeatedly or persistently takes part in firing it, some growth process or metabolic change takes place in one or both cells such that A's efficiency, as one of the cells firing B, is increased.

The Hebbian rule establishes the important relationship of the connections between the elements of the system (neurons), and provides the foundation of “synaptic plasticity”—the variation of the weight function of the signal transmittance from the axon of one neuron to the dendrite of the other neuron as the function of the frequency of the utilization of this particular synapse (transmission point). Biological nervous systems have the possibility to reinforce these junctions or to inhibit them. Such behavior

is the basis for the so called “supervised” and “unsupervised” learning. At the physiological level, probably it is difficult to make a difference between these types of learning, therefore, the current status of the terminology in this field reduces both of them to “unsupervised learning.” In fact, even if the external training helps to come faster to a certain conclusion, the conclusion itself will be reached by the “object” itself according to its free will and certain environmental conditions allowing a more probable pathway from each bifurcation point.

Even if there are several models describing learning in biological systems,<sup>2</sup> all of them take into account the synaptic plasticity phenomenon, by varying the connections between non-linear elements. Some models include also the variations of the nonlinear elements properties as well, even if this behavior is still currently under the discussion.<sup>3,4</sup>

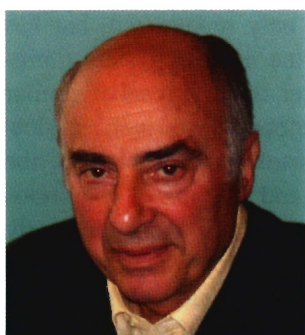
Summarizing, we can claim that the essential part of the natural nervous systems is based on the presence of synapses, allowing to modify signal pathways between non-linear elements (neurons) according to previous experience. Disregarding for the moment the possible modification of the individual neuron properties, we can claim that synapses are essential for learning and memory of the system.

Considering the spatial scale,<sup>5</sup> we can see that neurons, as also the most of other cells, have dimensions in the range of several microns. These micron sized objects can be connected with “wires” of even up to cm range in length. Apparently, natural objects avoid nm elements for the realization of the most complicated known systems. However, more detailed consideration would allow to find

**Victor Erokhin** is a senior scientist in Institute for Chemical and Physical Processes (National Council of Research, Italy) in a close collaboration with University of Parma. He is an author of about 120 scientific publications and 8 patents. His main activity was related to thin films of biological molecules and quantum effects in space confined systems (nanoparticles). After 2005, the main interest is in the field of bio-inspired adaptive systems.



**M. P. Fontana** is professor of Experimental Physics at the University of Parma, Italy. He is author of about 190 publications in the fields of spectroscopy of disordered systems, soft matter, Langmuir-Blodgett films, molecular electronics. Particularly interesting are his studies on optical properties of color centers in ionic solids, vibrational spectroscopy of liquid crystals and superionic materials. More recent work involves fabrication and characterization of complex polymeric structures for bio-inspired information processing systems.



contradictions in the statement presented above. In fact, a lot of fundamental processes take place in biological membranes—about 5 nm thick boundary elements separating the elementary “living units” from the environment. Nervous cells are not exceptions. Important processes, such as ionic transport, responsible for the trans-membrane potential generation, that is finally the elementary “bit” of the spreading information, take place within these objects. Thus, even if the spatial dimensions of the main functional units are well beyond the nm range, these units are fundamentally “nano-engineered” ones. It means that their essential components must be well-resolved and mutually arranged at the nm level.

The aim of the present short review is to give some ideas on the possible approaches on the realization of a bio-inspired material system, capable of learning and, to some extent, of decision making.

Modern electronics provides a wide variety of non linear elements, that can be used, after special modification and organization in circuits, as neuron analogs. However, direct analogs of synapses are not available among the existing electronic compounds, with the only exception being the hypothetical “memristor,” proposed theoretically by Chua in 1971.<sup>6</sup> An essential feature of this element is that its resistance must be a functional of the current which has passed through it. Such behavior corresponds well to the property, described by the Hebbian rule, presented above.

The present work is organized in the following way. After the present introduction, we will describe in the second chapter the concept of the memristor. First, we will consider the main ideas of Chua, claiming the principal reasons for the element occurrence. In the same chapter we will discuss the main modern experimental achievements in the field of memristors.

As the working principle of the organic memristor is based on the redox processes, occurring in conducting polymers, the next Chapter (3) will be dedicated to the molecular electronics elements based on electrochemical processes. We will overview the state of the art in the field starting from 1980ies, where first electrochemical field effect transistors have been reported.

The fourth chapter will describe the electrochemical hybrid polymeric element, reported for the first time in 2005, and recognized as memristor in 2008. We will describe the element architecture, its main properties, basis for the possibility of the adaptive networks construction. In addition, we will show that, up to our knowledge, it is the only experimentally described element, where the conductivity is directly connected to the transferred charge.

The fifth chapter will be dedicated to a special feature of the organic memristor—possibility to generate current–auto oscillations at fixed external bias voltage.

The sixth chapter will give examples of the adaptive networks, mimicking to some extent both supervised and unsupervised learning, realized using these organic memristors as key elements.

The seventh section will describe alternative approaches, where the networks are fabricated not by the deterministic arrangement of the elements, but by using auto-organization processes, such as, for example, fibre formation capabilities.

Finally, in the conclusions section we will try to draw perspectives and the main problems that must be resolved to arrive at a new computational hardware paradigm, that can allow, first, to understand better ourselves (brain and mind mechanisms) and, second, to establish, in the case of success, new principles and architectures for the next generations of computers.

## 2. MEMRISTOR

Ethymology of the word “memristor” implies that the element combines the properties of the resistor with memory. It means that the resistance is not fixed but it is a function of the memorized events connected with the signal transmitting process during the past operation.

Originally, the concept of the “missed” passive element was introduced considering symmetry reasons. Four fundamental parameters of electronic circuits were considered: voltage, current, charge, and variation of the magnetic flux. Instead, only 3 passive elements of electronic circuits are known to connect these fundamental parameters with each other. Resistance is the property of the material establishing the relationship of the current value with the applied voltage. Capacitance is the coefficient relating the voltage with the accumulated charge, and the inductance links the current with the variation of the magnetic flux. The missed element, introduced by Chua, must provide a relationship between the charge and the variation of the magnetic flux.<sup>6</sup> A practically important particular version of the element can be described as a resistor with variable resistance according to the following Eq. (1):

$$V = R(w)i \quad \frac{dw}{dt} = i \quad (1)$$

where  $V$  is voltage,  $i$  is current,  $R$  is memristance (variable resistance) and  $w$  is a parameter, whose derivative is equal to the actual current value.

Momentary variation of its resistance is directly connected to the current in this particular moment and, therefore, the actual resistance value is a function of the charge, transferred through it. This property has given the name for the element—memristor = resistor with memory.

As it has been mentioned by Chua in the same work, the mentioned electronic properties could be reached using already existing traditional elements by combining them in a special circuit. As an example, Chua has suggested the circuit whose scheme is shown in Figure 1. As it is clear from the figure, the circuit must be rather complicated and it must involve several active elements. Considering that even rather simple biological nervous systems

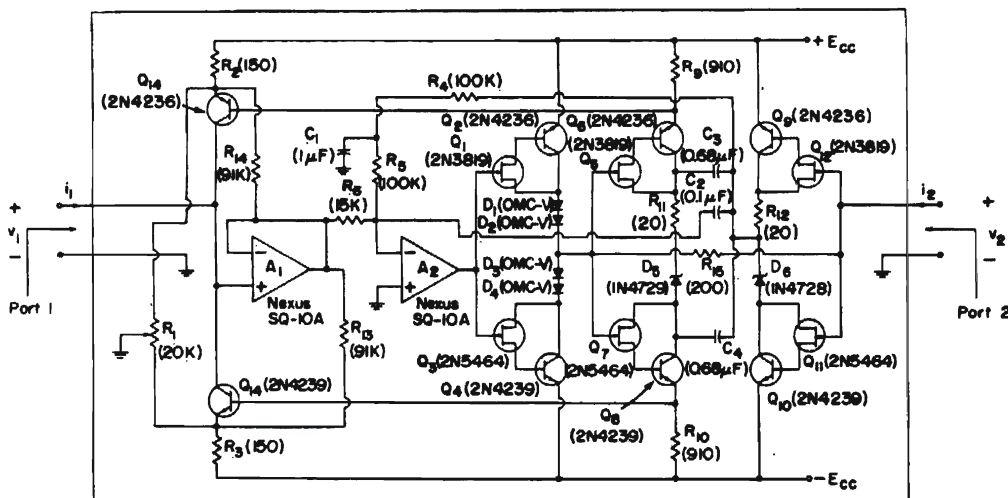


**Fig. 1.** Active circuit performing memristor function. Reprinted with permission from [6], L. Chua, *IEEE Trans. Circuit Theory* 18, 507 (1971). © 1971, IEEE.

involve a large number of synapses, their mimicking with elements, represented by the scheme shown in Figure 1, seems a very difficult task. If consider brain with its millions of synapses, technological resolving of the task will be practically impossible. Therefore, the challenge was to realize the single element, capable to perform the same function. Successful realization of this element would simplify significantly the problems of the realization of networks, capable to reproduce some brain properties, such as learning and decision making.

A seminal work in this field has been published in 2008. A two-electrode element with  $\text{TiO}_2$  as an active medium has been proposed and realized.<sup>7</sup> Hysteresis of the electrical characteristics, observed in the element, has been attributed to the drift of positively charged oxygen vacancies acting as native dopants.<sup>8</sup> However, direct connection of the element resistance with the transferred charge, a key property of the hypothetical memristor, was not observed. Moreover, the presented experimental data have demonstrated not the gradual variation of the element conductivity, but a bistable behavior of this value. Initially low conducting element was transferred into the more conducting state when the applied voltage went over a certain level. The element remained in the high conducting state during the back scan of the voltage and switched to the low-conducting state after reaching a certain negative voltage value. In a more recent paper the claim is made that the junction behaves as a memristor only within a certain voltage range.<sup>9</sup> Later, another mechanism for the memristor properties was suggested:<sup>10</sup> “necessary and enough” for explaining the properties of the described element is the redox transformation of titanium in the active  $\text{TiO}_2$  layer, responsible for the significant difference in the conductivity. Even if it is possible to find similar properties between oxygen vacancies drift and redox reaction, it seems that the explanation given in Ref. [10] is more correct.

However, the cited work had the merit of stimulating a great increase of the experimental activity in the field of

the memristors. Let us present some numbers: 18 journal articles were published in 2008 after the cited paper, and the number of published works increased to 60 in 2009. However, in most of the papers the authors report the conductivity switching rather than its gradual variation.

In most of the works the active layers were fabricated from metal oxide materials, such as  $\text{Gd}_2\text{O}_3$ ,<sup>11</sup>  $\text{VO}_2$ ,<sup>12</sup>  $\text{Fe}_3\text{O}_4$  nanoparticles.<sup>13</sup> However, successful realizations of the Si-based memristive systems were also reported.<sup>14</sup> In molecular layers, mechanisms responsible for the conductivity switching were attributed to the electronic and ionic charges at the boundary with metal electrodes.<sup>15</sup> The possibility of the realization of spin memristor has been also reported.<sup>16</sup> Finally, the possibility of the realization of logic elements, based on memristor systems, is also discussed.<sup>17, 18</sup>

### 3. ELECTROCHEMICAL ELECTRONIC ELEMENTS

Redox reactions are among the most important for the metabolism of living beings, including processes occurring in the nervous system and responsible finally for the treatment of information from sensorial systems, memory, learning and decision making.

In the case of traditional electronic devices, the field-effect transistors, based on redox reaction, have been reported in 1980ies.<sup>19</sup> The working principle was based on the difference of the conductivity of some compounds in the reduced and oxidized states. Scheme of the example of the realized electrochemical field-effect transistor is shown in Figure 2.

Even if the possibility of realizing the transistor, as well as the possibility of its utilization for sensors,<sup>20</sup> has been demonstrated, the activity in this field was limited mainly to academic research. In fact, the requirement of the utilization of liquid medium as electrolyte, necessary for the

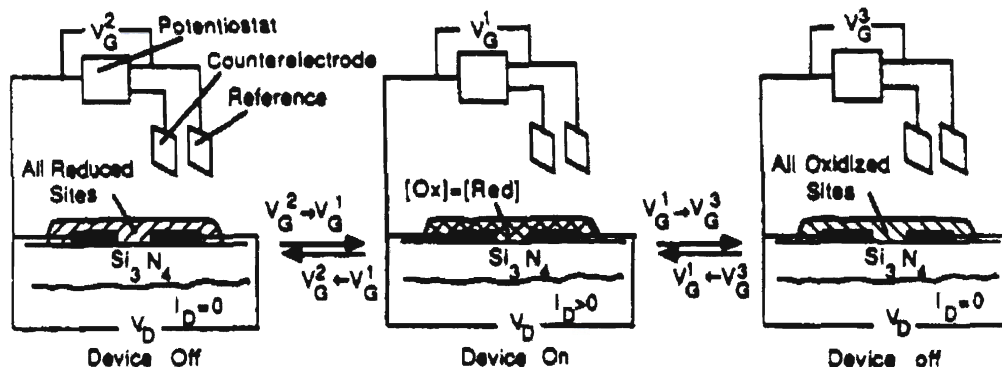


**Fig. 2.** Microelectrochemical transistor based on a conventional redox polymer. Reprinted with permission from [19], C.-F. Shu and M. S. Wrighton, *J. Phys. Chem.* 92, 5221 (1988). © 1988, American Chemical Society.

redox reactions, has restricted significantly the application of the electrochemical principles for the realization of real electronic components, suitable for the construction of commercial devices.

Nevertheless, some activity continued and has resulted in the accumulation of the knowledge in the field.<sup>21,22</sup>

An important paper was published in 2002.<sup>23</sup> It describes the fabrication of 2-terminal element with rectifying electrical characteristics. It is important that the described device does not require liquids—the electrolyte is also solid, a polymer-based matrix with dissolved lithium salt. Moreover, this paper describes 2-electrode system with non-linear properties based on electrochemical transformations, which is not a trivial technical solution. In fact, when we are working with electrochemical reduction or oxidation processes, we need to apply adequate potentials for starting these reactions. In the case of electrochemical FET, we have the third electrode—reference electrode—providing the reference point for the potential. In the 2-terminal element, instead, each electrode can be considered as the reference one for the other. Thus, for practically any bias voltage, we can expect that the reduction conditions will be satisfied for the active organic material in contact with one of the electrodes (more negative). Considering that for the most of materials in general, and in particular for the prototype conducting polymer—polyaniline, that we will consider later in more detail, the reduced state is practically insulating, any significant bias

of the junction will result in its transformation, as a whole, to an insulating state.

This difficulty has been resolved by a very specific geometry of the realized element. Its scheme is shown in Figure 3.<sup>23</sup> It has demonstrated a rectification of the electrical signal. Later, the developed approaches have been applied for the formation of other electronic components,<sup>24,25</sup> including logic elements.<sup>26</sup> We would like to underline that the work was the direct prototype for the development of the research that has resulted in the realization of organic memristor.

#### 4. ORGANIC MEMRISTOR

In 2005 the paper describing polymeric non-linear electrochemistry-based element has been published.<sup>27</sup> Even if in the initial publications the element was not defined “memristor,” its properties are very close to that of the hypothetical one. Let us consider its architecture and basic properties.

The scheme of the organic memristor is illustrated in Figure 4.<sup>28</sup>

An insulating support with two metal electrodes was used as the substrate for the deposition of the active channel, an ultrathin film of polyaniline (PANI). Similarly to the electrochemical FET, the working principle of the memristor is also based on the drastic difference of

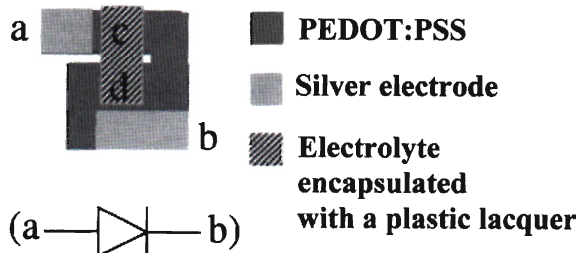


**Fig. 3.** Top view of the electrochemical rectifier. Reprinted with permission from [23], M. Chen et al., *Appl. Phys. Lett.* 81, 2011 (2002). © 2002, American Institute of Physics.

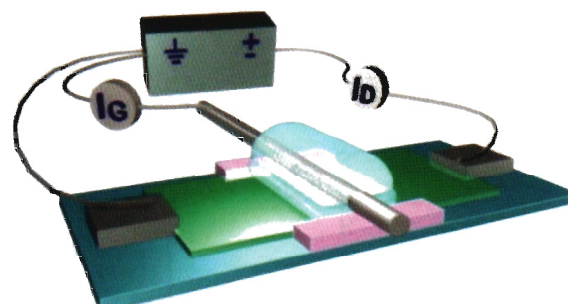


**Fig. 4.** Schematic representation of the organic memristor with external power supply and measuring devices. Reprinted with permission from [28], T. Berzina et al., *J. Appl. Phys.* 105, 124515 (2009). © 2009, American Institute of Physics.

conductivity of the conducting polymers in general, and PANI in particular, when they are in the reduced or oxidized state. For PANI, the diagram of reactions, responsible for the conductivity states, is shown in Figure 5.<sup>29</sup>

Emeraldine base form of PANI is the initial form of the material, from which the active channel is formed. There are two reasons for the beginning with this PANI form. First, the material is well processable and allows to form even very thin molecular layers. Second, even if the form itself is insulating, it can be easily transferred into the conducting form by doping, usually, with acid treatment as it is shown in the same Figure 5 (HCl treatment is shown here as the more frequently used case). The doping results in the attachment of a proton to the polymeric chain, as it is shown in the Figure 5. As a result of such modification of the polymer chain structure, there is a lack of the electron in the molecule (the conductivity of the most of conducting polymers is of *p*-type) that must be compensated by the electrostatic coordination of counter-ion ( $\text{Cl}^-$ —in this particular case) to the polymeric chain. The conductivity of the PANI after doping is really high. Maximum conductivity reported in the literature can reach  $1000 \text{ S cm}^{-1}$  or even more.<sup>30</sup> However, in our experiments this value was in the range of  $1\text{--}30 \text{ S cm}^{-1}$ , which is already high enough for the realization of devices that can be used also for real industrial applications. In our earlier experiments we have used HCl as a doping agent. However, recent results,<sup>28,31</sup> with the preliminary doping performed with dodecyl benzene sulfonic acid (DBSA), has resulted in the significant improvement of the channel conductivity and also shifts of the reduction potential to the negative values, which is due to the slightly acid nature of the used material.

The main reversible reaction, responsible for the organic memristor functioning is shown in the right part of the

same Figure 5. The conducting form of PANI can be transformed into the insulating form by the reduction of the material if the adequate reduction potential is applied. It is very important that the reaction is reversible: the material will be transferred again into the highly conducting form after the application of the appropriate oxidation potential to it. The choice of the mentioned reaction implies an essential requirement for the thickness of the active channel. As the reactions involve the movement of ions, the process is a diffusion-controlled one. Therefore, the thickness of the channel must be rather low, allowing the effective conductivity transformations through the whole thickness within reasonable short time intervals. In fact, in our experiments the channel thickness was varied within the range of 24–100 nm.

Let us consider again the memristor configuration, shown in Figure 4. It contains two electrodes, connected through the active material (PANI), in which the conductivity variations take place. However, as the nature of these conductivity variations is due to redox reactions, there must be a medium allowing these reactions, i.e., the electrolyte. Taking into account all the drawbacks listed in the previous chapter, we must use solid electrolytes if we plan to realize elements which are suitable for the circuits of real devices.

Polyethylene oxide (PEO) is a well-known matrix of solid electrolyte that has demonstrated the adequate properties, especially used for super capacitors<sup>32</sup> and rechargeable batteries fabrication.<sup>33</sup> Lithium salts were used as the ionic dopants. The simplest lithium salt, namely  $\text{LiCl}$ , has not been considered as it is extremely hygroscopic and the electrolyte was always in the gel form. Initially, we have started with  $\text{LiClO}_4$ . More recent works were based also on other lithium salts, such as  $\text{LiBF}_4$ .

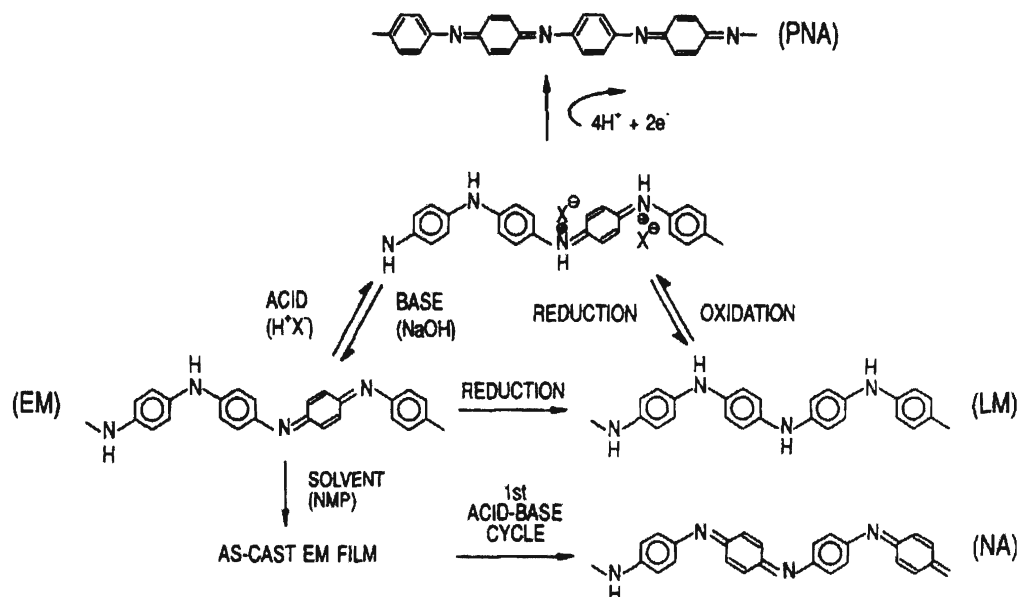


**Fig. 5.** Interconversions among the various intrinsic oxidation states and protonated/deprotonated states in polyaniline. Reprinted with permission from [29], E. T. Kang et al., *Progr. Polym. Sci.* 23, 277 (1998). © 1998, Elsevier.

The properties of the device were found to be somewhat dependent on the choice of the dopant salt.

A stripe of solid electrolyte was deposited in the middle part of the PANI channel. All redox reactions and, therefore, the conductivity variations can occur only in the PANI area in the contact with the electrolyte. Therefore, we will refer to this area as the “active zone” henceforth.

However, as we plan to use the electrochemical redox transformations for the conductivity variations, we need one more essential element of the device—the potential reference point. Therefore, a third electrode, a silver wire, is placed into the electrolyte stripe.

One of the two metal electrodes, referred to as the source electrode (S), and the silver wire in PEO, which may function as a gate or a reference electrode (G), are connected to the ground potential level, while the second metal electrode at the substrate, the drain electrode (D), is biased by the external voltage unit. The shorting of the gate and source electrodes is a very important point as the reference electrode is maintained at zero potential and all redox reactions occur according the actual potential of the active zone with respect to this zero potential. Such configuration turns the element into an effective two terminal device. Electrical connections of the element to the external circuit are also shown in Figure 4, where the position of the amperometers, measuring drain and gate currents are indicated. Gate current is a ionic current in the electrolyte, while the drain current is a sum of the ionic current in the electrolyte and the electronic current in the PANI channel. Thus, in discussing mechanisms of the memristor functioning, it is useful to present also the difference current (drain – gate) that will illustrate better the variation of the electronic conductivity in the active zone of PANI.

Cyclic voltage/current (V/I) characteristics for drain, gate and difference (drain – gate) currents are significant parameters of the element. Typical characteristics are shown in Figure 6.<sup>27</sup> The reported characteristics were acquired on the freshly fabricated device. The presence of non-zero current values at 0 V is connected to the fact that transient processes occur after its connection to the external circuit. Instead, if the device was maintained at 0 V for 10–15 min, these transient processes were over and one can see  $I = 0$  A at  $V = 0$  V. Typical characteristics of the equilibrated element are shown in Figure 7. Sharpness and to some degree the position of the current peaks, corresponding to the reduction and oxidation processes, in the characteristics for the ionic currents, shown in Figures 6(b) and 7(b) depends on the time delay between the voltage application and the current acquisition. The presented dependences were obtained when 1 min delay was used between the voltage application and the current measurements.

Measurements are usually started at 0 V and increase with the increment of 0.1 V (of course, these values can be varied). 1–3 minutes delay is applied at each value of the

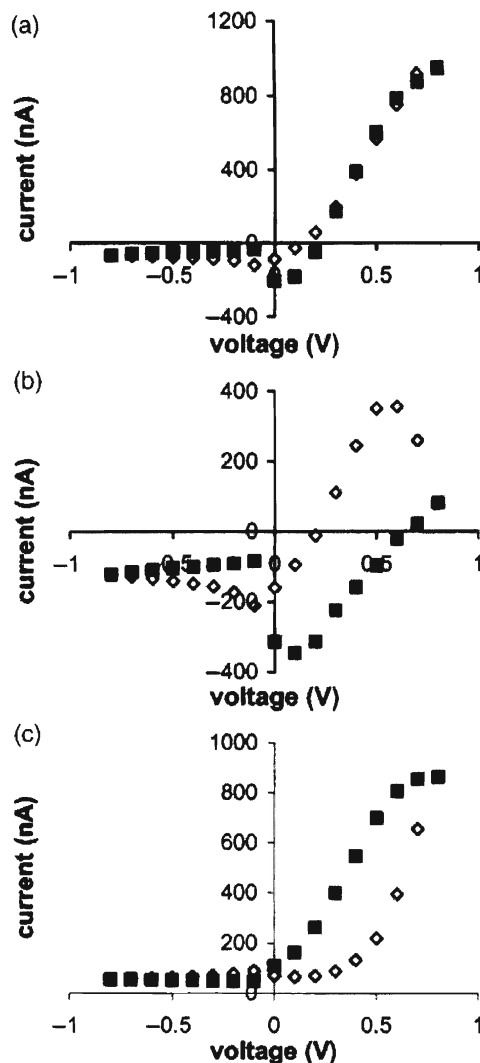


**Fig. 6.** Drain (a), gate (b), and difference (c) current dependences upon drain voltage. The empty rhombs represent increasing voltage branch and the filled squares represent decreasing voltage branch (in absolute value). Characteristics were obtained from the pristine device. Reprinted with permission from [27], V. Erokhin et al., *J. Appl. Phys.* 97, 064501 (2005). © 2005. American Institute of Physics.

applied voltage before the acquisition of the current value to equilibrate electrochemical processes. Let us mainly consider the characteristics, shown in Figures 6(b and c) (as well as in the Figs. 7(b and c)), corresponding to the ionic and electronic currents respectively. If the memristor is initially in its insulating state (it can be done by the conditioning of the element at 0 V for rather long time (10–20 min) before the V/I characteristics measurement), the initial increase of the applied voltage results in a small variation of both ionic and electronic currents. This feature is more clearly visible in the characteristics shown in Figure 7, as the element was conditioned at 0 V, while that corresponding to the Figure 6 characteristics, was an element immediately after the fabrication. After a certain value of the applied voltage (+0.5–+0.6 V in the particular cases, shown in Figs. 6 and 7) we can observe a significant increase of the ionic current and reaching of its

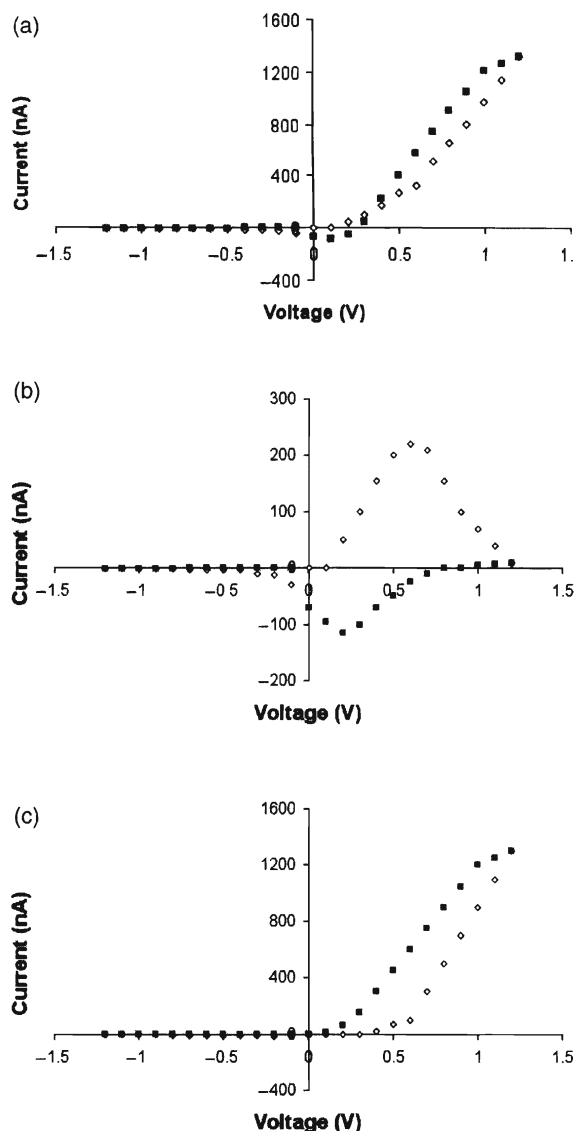


**Fig. 7.** Drain (a), gate (b), and difference (c) current dependences upon drain voltage. The empty rhombs represent increasing voltage branch and the filled squares represent decreasing voltage branch (in absolute value). Characteristics were obtained from conditioned device.

maximum value. The applied voltage at which the maximum is observed corresponds to the oxidation potential of PANI in the active zone. In fact, reaching this value we can observe a significant increase also in the electronic current. Maximum positive value of the applied voltage is usually limited by +1.2 V, as undesirable processes of irreversible overoxidation, resulting in the significant decrease of the memristor conductivity, occur after the application of more than +1.5 V. After reaching the maximum, the applied voltage begins to decrease with the same increment and delay time. We can observe high electronic conductivity of the memristor. At a certain value of the applied voltage (+0.1 V) we can see that the ionic current reaches its minimum value, corresponding to the reduction of PANI in the active zone. After passing this value, significant decrease of the electronic conductivity also occurs. Increase and

decrease of the applied voltage in the negative branch is characterized by low conductivity for both ionic and electronic currents.

Other important characteristics, reporting the variation of the total memristor conductivity in time at fixed values of the applied voltage are shown in Figure 8 for +0.6 V (1) and -0.1 V (2).<sup>34</sup> As it is clear from the figure, we observe the increase of the conductivity for the positive voltages up to the oxidation potential and the decrease of the conductivity for any negative voltage. Both processes are coming to saturation levels but with different kinetics. In our initial works, the ratio in the conductivity for the memristor in oxidized and reduced states (saturation levels) was about 2 orders of magnitude. Optimization of the materials and the device construction have allowed to increase this ratio to 4 orders of magnitude.<sup>28,31</sup>

The characteristic (1) in Figure 8 can be considered as a direct analog of an element governed by the Hebbian rule. The conductivity of the memristor for a positive bias is a function of its involvement in the signal transferring process. Therefore, this property can be the basis of the unsupervised learning. The dependence (2) in the same Figure 8, instead, can be the basis of supervised learning as it gives the possibility to inhibit occasionally formed signal pathways by adequate external action (training), based on the application of negative bias voltage between corresponding input–output pairs. In addition, short term application of the negative voltage between all input–output pairs will prevent the system, from reaching the saturation, when further increase of the conductivity would be impossible.

The difference in the kinetics for oxidation and reduction processes is a very interesting feature of the conductivity variation. However, before explaining this phenomenon, let us consider in more detail the mechanisms responsible for the organic memristor behavior.

In order to understand these mechanisms, first experiments were performed using microRaman spectroscopy.<sup>34</sup> A set of spectra, acquired in the same point of the active zone in the memristor, maintained at different voltages for different time, are shown in Figure 9. The peak at

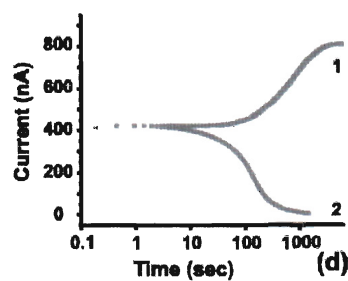


**Fig. 8.** Typical temporal dependences of the drain current at fixed applied voltages: +0.6 V (1) and -0.2 V (2). Reprinted with permission from [34], T. Berzina et al., *J. Appl. Phys.* 101, 024501 (2007). © 2007, American Institute of Physics.

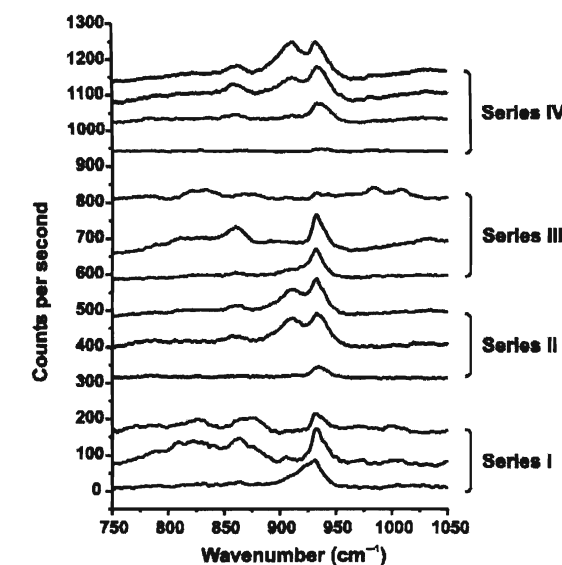
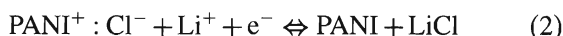


**Fig. 9.** Raman spectra from the PANI-PEO heterojunction under the cyclic application of the voltage of different polarity. Series I:  $-0.2\text{ V}$  with curves from bottom to top, immediately after voltage application, after 15 and 30 min. Series II: at  $+0.6\text{ V}$  with curves from bottom to top after 2, 5, and 30 min. Series III: at  $-0.2\text{ V}$  with curves from bottom to top after 2, 20, and 60 min. Series IV: curves from bottom to top after 2, 20, 30, and 60 min. Reprinted with permission from [34], T. Berzina et al., *J. Appl. Phys.* 101, 024501 (2007). © 2007, American Institute of Physics.

$930\text{ cm}^{-1}$  is of a particular interest.<sup>35</sup> Lithium perchlorate was used as the dopant for our electrolyte. The presence of a single peak at this wavenumber value corresponds to the presence of  $\text{ClO}_4^-$  ions whereas its splitting into two peaks corresponds to the formation of the lithium perchlorate complex. As it is clear from the figure, negative bias of the memristor results (after some time necessary for the reaction) in the splitting of the  $\text{LiClO}_4$  complex into ions.  $\text{Li}^+$  ions leave electrolyte and react with  $\text{Cl}^-$  ions, initially associated with PANI molecules in emeraldine salt oxidized form, and detached during the reduction. For the successive positive bias, the PANI is oxidized, attaching electrostatically  $\text{Cl}^-$  ions, and  $\text{Li}^+$  ions are displaced back to the PEO matrix, reconstituting lithium perchlorate complex.

Summarizing, the reaction responsible for the conductivity variation of the organic memristor can be shown in the following way (2):<sup>36</sup>



More direct measurements, confirming the proposed scheme of the conductivity variations were obtained by time resolved simultaneous measurements of the electrical characteristics and X-ray fluorescence using grazing incidence synchrotron radiation for the excitation.<sup>37</sup>

X-ray fluorescence is a powerful tool allowing time resolved study of the ion motion at interfaces.<sup>38</sup> However, lithium fluorescence energy cannot be detected at atmospheric conditions. Therefore, lithium must be substituted

with heavier ions. We have chosen rubidium, as it is also a monovalent metal and it provides well resolved fluorescent spectrum lines. However, this choice required also changes in the memristor construction. In fact, in the case of  $\text{Li}^+$ , we have used the solid electrolyte, while it was impossible for  $\text{Rb}^+$  because of very low ion mobility. Therefore, for these measurements we have used PEO based electrolyte in the gel form. Scheme of the measurements and photo of the experimental cell are shown in Figure 10. Thin layer of kapton—inert insulating material—was used as a support, where PANI channel was deposited. The support with the layer was placed onto the teflon box with the well filled with  $\text{RbCl-PEO}$  gel (PANI deposited side in the contact with the gel). Two contacts to PANI were made with Al electrodes, while the reference electrode (silver wire) was placed in the well with the electrolyte. Measurements were performed following the voltage variation as it has been done for the memristor characteristics shown in Figure 6 and discussed above.

The measurements have shown that the conductivity of the memristor is directly proportional to the integral of the gate current (transferred ionic charge). Let us recall that it corresponds well to the Chua suggestion (1) with the only difference that the resistance is a function of not the total

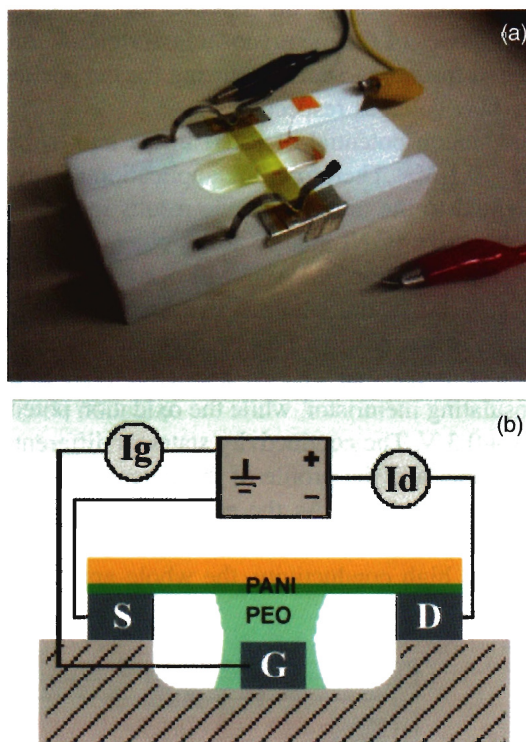


**Fig. 10.** Experimental setup (a) and scheme of electrical connections (b) for X-ray fluorescence measurements. The thickness of the PANI layer is about 110 nm, the length of the active zone is 1.5 cm, the width of the active zone is 1.0 cm, and the depth of the well (gel electrolyte thickness) is 1.0 cm. Reprinted with permission from [37], T. Berzina et al., *ACS Appl. Mater. Interfaces* 1, 2115 (2009). © 2009, American Chemical Society.

current but its ionic component (3). Ionic component of the total current is shown as  $i_{\text{ion}}$  in Figures 4 and 10.

$$\begin{aligned} v &= R(w)i_{\text{tot}} \\ \frac{dw}{dt} &= i_{\text{ion}} \end{aligned} \quad (3)$$

According to our knowledge, up to now this is the only work where such relationship has been directly demonstrated.

Concerning the dependence of the resistance on the total current, passed through the device, the relationship is not such direct one. In fact the value of the resistance can be varied only within certain limiting values, corresponding to the reduction of the whole amount of PANI in the active zone (maximum resistance) or oxidation (minimum resistance). Furthermore the variation of the actual PANI redox state and, therefore, the memristor conductivity can start only when the applied voltage provides the appropriate potentials in the active zone. Some discussions on these facts will be presented later considering the model of the memristor working principles.

A scheme, illustrating the ion motion in the device is shown in Figure 11 and it confirms even more directly than the microRaman data the reaction Scheme (2) where Li ions must be substituted by Rb ions.

Now, let us consider the reasons of the difference between kinetics of the memristor transformation into conducting and insulating states occurring for the positive and negative bias voltages respectively.

The reduction potential of PANI in the bulk conditions is about +0.1 V.<sup>39</sup> Therefore, the application of any negative potential to the drain electrode results in the fact that the whole active PANI area is at the potential lower than +0.1 V and reduction of PANI will occur simultaneously for the material in the whole active area. In the case of application of the positive potential the situation is different. Let us suppose that we have applied +0.6 V to the initially insulating memristor, while the oxidation potential of PANI is +0.3 V. The conductivity states of different zones of the channel and the profile of the potential along it are shown in Figure 12(a). As the active area is in the insulating state, and zones of PANI not covered by electrolyte have always high conductivity, the whole applied voltage

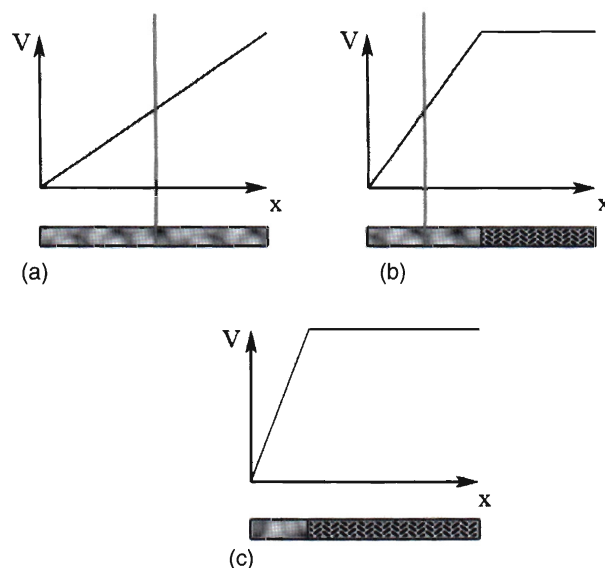


**Fig. 12.** Potential distribution profile and the state of PANI in the active zone after application of +0.6 V.

is mainly distributed in the active zone, as it is shown in Figure 12(a). Therefore, only about the half of the PANI length in the active zone, closer to the drain electrode, will be biased by the potential higher than the oxidation one, allowing, therefore, its transformation into the conducting state. After the transformation, the right segment of the initially insulating part of the active area will be transformed into the conducting state and, therefore, the profile of the applied potential along the PANI channel will be redistributed, as it is shown in the Figure 12(b). Thus, the applied +0.6 V will be mainly distributed on the half of the active zone, and the half of it, again, closer to the drain electrode, will be at the potential suitable for the PANI oxidation. Therefore, the next step will be the transformation of this area into the conducting state. The consideration can be continued till the oxidation of the whole active zone.

Summarizing, qualitative considerations can explain the difference in the kinetics of the memristor transformation from the conducting state to the insulating one and vice versa by the fact that in the first case the transformation takes place for the whole active area and depends on the diffusion coefficients only, while in the second case it

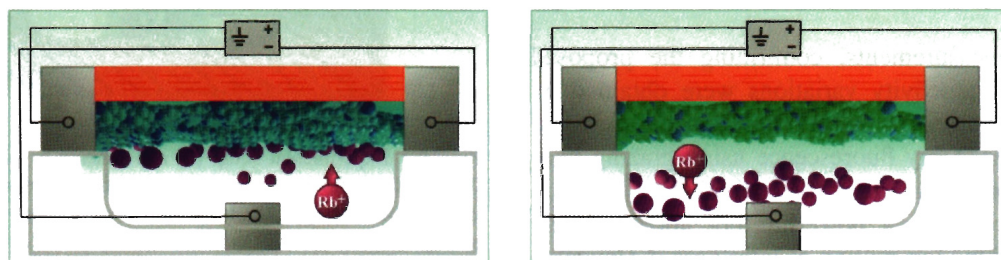


**Fig. 11.** Scheme of the process occurring in the structure for negative (left) and positive (right) applied voltage. Reprinted with permission from [37], T. Berzina et al., *ACS Appl. Mater. Interfaces* 1, 2115 (2009). © 2009, American Chemical Society.

occurs gradually: only a part of the active zone is under the conditions suitable for the transformation for each fixed time moment. When the transformation takes place, other parts of the active zone begin to satisfy the conditions for their transformation into the conducting state. In other words, for the negative bias we have simultaneous transformation of the active PANI area into the insulating state, while for the positive bias we can observe a gradual displacement of the conducting parts of the active layer in the direction from the drain to the source electrodes.

Quantitatively, the mechanism has been described by the following model.<sup>40</sup> The active area has been divided in narrow stripes (number of stripes and the width of each stripe were variable). It was supposed that the material within each stripe varies its properties simultaneously. Two potentials were considered as limiting ones: oxidation and reduction potentials.

Numerically, these values were +0.3 V for the oxidation and +0.1 V for the reduction, in correspondence to the PANI bulk properties.<sup>39</sup> Thus, the possible processes within the stripe were determined by its actual potential. We can distinguish several possible states of this potential (4):

- (1)  $V < +0.1 \text{ V}$
- (2)  $+0.1 \text{ V} < V < +0.3 \text{ V}$
- (3)  $V > +0.3 \text{ V}$

The second important feature of the model is the attribution of the internal timer for each stripe, which begins to count time determining the kinetics of the conductivity variation, when the actual potential of the stripe with respect to the reference potential passes from one above mentioned interval to the other.

Similarly to the case shown in Figure 6, we are going from the low (0 V) value of the potential to the higher ones (supposing that the initial state of the stripe is an insulating one). No conductivity variations are supposed to occur till some stripes arrive to the oxidation potential (+0.3 V). Once arrived, the timer of the stripe will be activated (attributing time “0” to the moment of the passing of this boundary value): the material within the stripe will begin to transform itself into the oxidized state according to the diffusion-controlled experimentally determined kinetics. Further increase of the actual potential of the stripe results only in the Ohmic variation of the output current. Reaching the maximum, the applied voltage begins to decrease, exhibiting also an Ohmic dependence of the current, till some stripes will arrive to the reduction potential (+0.1 V). Reaching this value, the timer of the stripe will be reactivated (assuming time “0” for the moment of the arrival) and the decrease of the conductivity will occur till the saturation. Thus, the memristor will be in its insulating state for the all negative branch of the applied voltage.

After fixed variable time intervals, the program recalculates the profile of the voltage distribution along the active PANI layer, determining the conductivity status of each stripe.

The results obtained with this model were found to be in a good quantitative agreement with experimental data.

## 5. AUTO-OSCILLATING MEMRISTOR

An essential feature of the living beings is the occurrence of rhythmic oscillatory processes even in fixed environmental conditions. This is the reason why the cyclic chemical reactions, such as well-known Belousov-Zhabotinsky (BZ) reaction,<sup>41</sup> became very popular immediately after first publications on this topic. They can explain fundamental features occurring in biosystems for the maintaining of life conditions. Recently, BZ reactions were considered also as a possible mechanism for the realization of alternative computers.<sup>42</sup>

Effective application of the memristor in bio-inspired electronic systems must provide also the possibility to obtain rhythmic electrical response in fixed bias voltage conditions, imitating somehow clock generation in traditional computers.

As the memristor construction implies only two terminals for the connection to the external circuit (ground and bias voltage), the only possibility to have oscillating behavior is to modify the element construction in such a way, that the reference potential will not be fixed anymore. This can be done by the connection of an external capacitor between the gate and source electrodes,<sup>43</sup> as it is shown in Figure 13. In such configuration, the ionic flux in the active zone between the conducting polymer and solid electrolyte will result in the charging-discharging cycles of the capacitor and, therefore, in the variation of the reference potential.

Experimental temporal dependencies of the drain and gate currents at the fixed value of the applied potential are

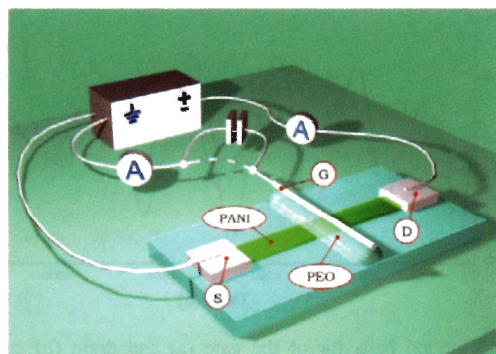


**Fig. 13.** Scheme and connections of the organic memristor for the generation of current auto-oscillations. In the case of graphite gate electrode, the external capacitor is absent. Reprinted with permission from [43], V. Erokhin et al., *J. Phys. Condens. Matter* 19, 205111 (2007). © 2007, IOP Publishing Ltd.

shown in Figures 14(a and b), exhibiting rhythmic oscillating behavior. Oscillations of drain and gate currents are shifted in phase, as shown in Figure 14(c).

Application of the above model<sup>40</sup> to such system has resulted in a good qualitative agreement with the observed experimental results.

It is necessary to consider two interconnected processes for the qualitative explanation of the observed oscillations. The first process is connected to the motion of ions in the electrolyte, guided by the actual potential difference between the gate electrode and the active zone of PANI layer, resulting in the charging–discharging of the capacitor. The second process is connected to the variation of the conductivity distribution along the PANI layer covered by the electrolyte, according to the actual potential at each point in the direction from the S to D electrodes with respect to the reference potential at the gate electrode.

Thus, a qualitative explanation of the observed oscillations can be the following one. Let us consider for instance the situation when a negative potential is applied to the structure (Fig. 15). Application of the drain voltage results

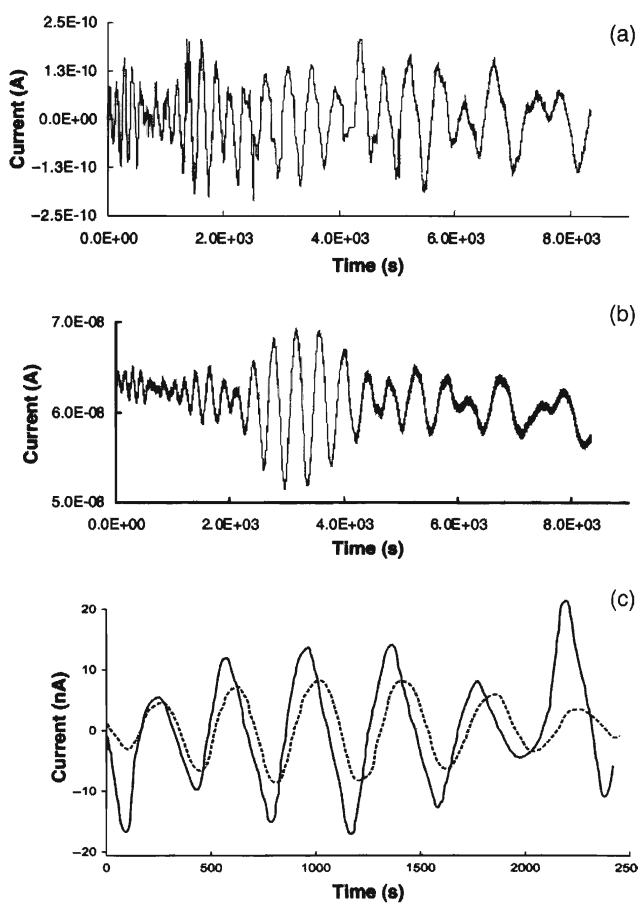


**Fig. 14.** Temporal behavior of the gate (a) and drain (b) currents in circuit with 1.0  $\mu\text{kF}$  external capacitor at a constant drain voltage of 1.0 V. Parts of both characteristics are shown in (c) for comparison (value of gate current (solid line) is multiplied by 100; value of the drain current (dashed line) is shifted by  $-0.5 \text{ nA}$ ). Reprinted with permission from [43], V. Erokhin et al., *J. Phys. Condens. Matter* 19, 205111 (2007). © 2007, IOP Publishing Ltd.

in a potential difference between the active PANI zone and the gate electrode. Initially, the whole active area of PANI has a negative potential with respect to the reference one, resulting in the transformation of this area into the insulating state. In parallel, charging of the capacitor takes place (Fig. 15(a)). After the transformation of the whole active area into insulating form (Fig. 15(b)), practically all applied drain voltage will be distributed within this area. However, the gate potential is not zero anymore, as it was varied due to the ionic gate current and it is negative with respect to ground. Therefore, zones of the active area closed to the source will reach an oxidizing potential with respect to the reference one. As a consequence, these zones start the transformation into the conducting form (Fig. 15(c)). After the transformation, these zones will be excluded from those where the most of the applied voltage is distributed. Thus, new zones, also closed to the source will be at an oxidizing potential with respect to the reference electrode, which will result in their successive transformation into the conducting form (Fig. 15(d)). These processes imply back motion of ions and, therefore, discharging of the capacitor. This process will be continued till the residual reduced insulating zones of the active area closed to the drain electrode will have the resistance comparable to the total resistance of the whole conducting area. The situation will be rather similar to that in the Figure 15(a) and the process will restart. Summarizing, two parallel, but strongly correlated, processes take place during the structure function. First, redistribution of the potential along the length of the active PANI area takes place (the most of the potential difference will be localized in the less conductive zone). Second, redistribution of the active layer conductivity will result in the fact that some areas at the junction will be at an oxidizing potential with respect to the gate electrode and a discharge of the capacitor will occur with back current flow to these zones. This ionic current will vary the conductivity profile along the active area, resulting in the new potential distribution. As we see from the Figure 14, gate current oscillations take place around zero value. Thus, in each time period there is a preferential direction of the ionic flow. Increase and decrease of the conductivity of the active area is connected to the direction of the ionic flow in the electrolyte. Phase difference of the oscillations of drain and gate current is connected to the fact that electronic conductivity of the active zone and, therefore, the drain current is a function of an integral of the ionic current.

It is possible to consider the observed results also from the other point of view, namely, to connect the observed phenomenon to the BZ reaction.<sup>41</sup> BZ reaction involves at least 3 processes: reactions of oxidation and reduction (one of them must be autocatalytic) and inhibition of the catalyser. In our case we also have redox reactions in the active area of PANI layer. Variation of the reference potential and redistribution of the potential profile along the length of

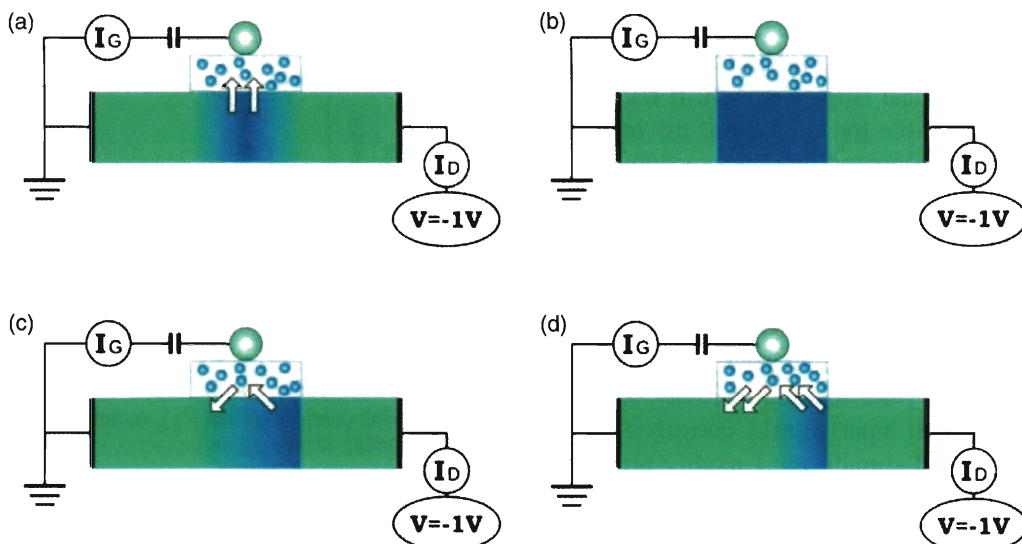


**Fig. 15.** Variation in conductivity of the PANI active area during device functioning (arrows indicate the opposite direction of  $\text{Li}^+$  flow). (a) After application of the negative potential, the active area begins to transfer into the insulating state simultaneously with capacitor charging. (b) The active layer is insulating, the capacitor is charged and the applied voltage is distributed mainly along the active area. (c) Zones of active area at the oxidizing potential begin to transfer into the conducting state, redistributing the potential profile. (d) Propagation of the conducting zones towards the drain until the resistance of the insulating zones is comparable with the total resistance of all conducting zones. Reprinted with permission from [43], V. Erokhin et al., *J. Phys. Condens. Matter* 19, 205111 (2007). © 2007, IOP Publishing Ltd.

REVIEW

the active zone can play the same role as processes responsible for the production and inhibition of the catalyster in BZ reaction.

These results have a particular importance. In fact, practically all previously published data on cyclic reactions in general, and BZ reaction in particular, were connected to the cyclic variations of optical and viscoelastic properties of the reaction medium. In the case of the organic memristor, instead, we have observed electrochemically controlled modulations of the electrical response, mimicking important features of biological systems.

The only drawback of the realized auto-oscillating system is the necessity of the utilization of an external electrical element—the capacitor. However, it turned out that the connection of the external element could be avoided. For this reason, the material of the gate electrode must be substituted with one which is capable to accumulate charges.

Highly oriented pyrolytic graphite is a well known material capable to perform such function. It is also widely used in studies on rechargeable batteries as an electrode, capable of charge accumulation. The small lithium ions can be intercalated between graphite atomic plates.

Thus, another element, capable of self-oscillation, was fabricated similarly to the normal organic memristor, shown in Figure 4. The only difference is that the silver wire, used as a reference electrode in the memristor, was substituted with a thin freshly cleaved layer of graphite. Temporal behavior of the current measured in such structures at fixed bias voltages is shown in Figure 16. Similarly to the circuit with external capacitor, the element shows rhythmic auto-oscillating behavior, demonstrating the possibility to avoid the utilization of additional external components and to have the effect with a single integrated element.

## 6. ADAPTIVE NETWORKS

The first circuit showing learning according to the homosynaptic plasticity mechanism has been realized with one memristor only. Learning of pond snail *Lymnea stagnalis* during feeding was taken as a biological benchmark.<sup>44</sup>

Learning of the snail implies the association of the mechanical stimulus with the presence of the food. In the case of the real animal, its lips were touched with sugar, after which the snail begins to open its mouth and starts the ingestion process after touching it even without sugar. For the untrained animal, instead, just mechanical touching does not result in any activity connected with feeding.

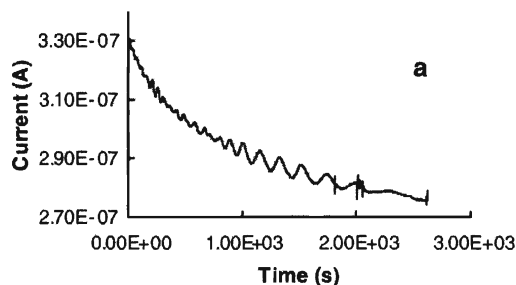


**Fig. 16.** Temporal behavior of the drain current measured in element with graphite electrode at drain voltage of +5.0 V. Reprinted with permission from [43], V. Erokhin et al., *J. Phys. Condens. Matter* 19, 205111 (2007). © 2007, IOP Publishing Ltd.

Designing the circuit, we have assumed that the system must have two inputs, corresponding to the mechanical (touching) and chemical (sugar) stimuli. It must have also one output, responsible for the start of the ingesting activities. We have also supposed that the execution of the activity can be performed only when the output signal will be higher than a certain threshold level.

The realized circuit must have the following properties. Initially, the application of the input signal, corresponding to the mechanical stimulus, must result in the output signal, lower than the threshold level and, therefore, not starting the analog of the ingestion activity. Simultaneous application of both input signals, corresponding to mechanical and chemical stimuli, must modify properties of the circuit in such a way, that successive application of only one input signal, corresponding to the mechanical stimulus, will result in the significant increase of the output, overcoming the threshold level and capable to start, therefore, the ingestion process.

A scheme of the circuit is shown in Figure 17.<sup>45</sup> Applied voltages (+0.3 V) each were taken as inputs, corresponding to both stimuli and connected to the summator unit that provides the voltage to the memristor. The current in the circuit was taken as the output signal. Initially, the memristor was in its low conductivity state. Application of each input signal alone was not enough for its transformation into the conducting state, while its simultaneous application provides the potential necessary for the PANI oxidation in the active zone.

Experimental results are shown in Figure 18. Initially (point 1 in the figure), only the input corresponding to the mechanical stimulus (MI) has been applied resulting in the appearance of steady state output current of about  $0.14 \mu\text{A}$ . Second input, corresponding to the analog of the chemical stimulus (TI = Training Input) has been applied at the moment corresponding to point 2 in Figure 18. Its application has resulted immediately in doubling of the initial value of the output. However, this current value is not constant anymore. We can see the increase of the output current in time, corresponding to the increase of the conductivity of the memristor. Point 3 in Figure 18 correspond to the moment when the input imitating the chemical stimulus was switched off. As it is clear from the figure, the output signal corresponding to the mechanical stimulus analog along was increased till the value of  $0.24 \mu\text{A}$ .

The presented results indicate the possibility to mimic synaptic plasticity and to realize adaptive circuits with

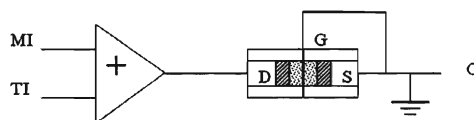


**Fig. 17.** Scheme (top view) of the learning circuit: MI—main input, TI—training input, +—summator. Reprinted with permission from [45], A. Smerieri et al., *Mater. Sci. Eng., C* 28, 18 (2008). © 2008, Elsevier.

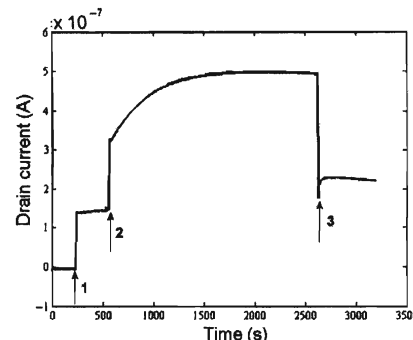


**Fig. 18.** Output current of the circuit in Figure 17 versus time [45]. Reprinted with permission from [45], A. Smerieri et al., *Mater. Sci. Eng., C* 28, 18 (2008). © 2008, Elsevier.

properties similar to those of the simple unsupervised learning. In fact, if we suppose that the threshold level of the function execution (mouth opening) is about  $0.2 \mu\text{A}$ , we can see that the application of the mechanical stimulus along to the “fresh” circuit will not start functioning. Instead, the conditioned circuit will be able to execute the function in the presence of the input, corresponding to the mechanical stimulus only.

A similar approach has been also applied to the system in the pulse mode, using sequences of the voltage pulses, which is much closer to the situation in the real biological systems where the information is propagated in the form of the spikes of potentials. The obtained results<sup>46</sup> were very similar to those presented here for the dc signals, indicating that the memristor can be used also in circuits operating in the pulse mode.

Next step was the demonstration of the possibility to realize a circuit capable of supervised learning.<sup>47</sup> The scheme of the circuit, containing 2 inputs, 2 outputs and 8 memristors is shown in Figure 19. As it is clear from the figure, there are several possible pathways for the signal to be transferred from each input to each output. As in the previous case, we have used applied voltages as inputs and current values near the output electrodes as outputs. In the case of the just assembled network, the application

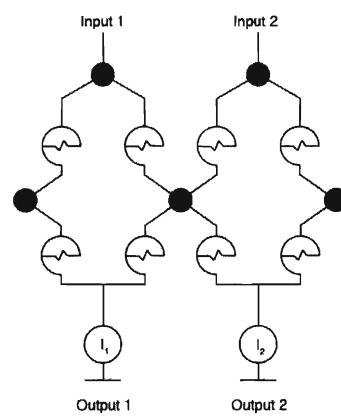


**Fig. 19.** 8-memristor based adaptive network capable to supervised learning.

of +0.5 V to the input 1 has resulted to the appearance of 0.5  $\mu$ A at the output 1 and 0.2  $\mu$ A at the output 2. The difference was due to the dispersion of properties of individual memristors, constituting the circuit. We have determined as a task of the supervised learning the reinforcement of signal pathways between input 1 and output 2 and the inhibition of those between input 1 and output 1. The training procedure was performed in the following way. A +1.2 V voltage was kept between the input 1 and output 2, while it was -0.5 V between input 1 and output 1, for 20 minutes. Testing of the system was performed applying again +0.5 V to the input 1 and analyzing the output currents. As the result of supervised learning due to the described training procedure, the output 2 signal was reinforced (from 0.2  $\mu$ A to 0.57  $\mu$ A), while the output 1 signal was inhibited (from 0.5  $\mu$ A to 0.15  $\mu$ A).

The presented results have directly demonstrated the possibility of supervised learning in memristor-based circuits. Reversible adaptations can be induced by the external training of the system with the application of adequate voltages between input-output pairs. We note that the circuit remains the same and its properties are varied just by the application of adequate training procedure.

Recent adaptive circuits with improved stability<sup>48</sup> were realized in the integral mode and on flexible supports.<sup>49</sup>

## 7. STATISTICAL NETWORKS

Realization of adaptive networks capable of learning, complex problem solving, and decision making demands circuits with millions of memristors, comparable to the number of neurons in the brain.

In modern microelectronics, the traditional approach is based on the utilization of technologies involving high-resolution lithography processes. This direct method minimizes the element sizes and increases significantly the complexity level of the system.

However, the modern fabrication techniques deal mainly with planar structures. In the brain, instead, we have 3D organization allowing also connections between rather distant neurons. Therefore, mimicking of the brain structure and function will demand the development of alternative approaches, i.e., to realize networks of memristors in 3D space.

We have started the search of new approaches by realizing fibrillar structures. The capability of the formation of fibers is well-known for some classes of polymers, PEO in particular. Electric field induced thinning is one of the most frequently used methods for this reason.<sup>50</sup>

In our work we found better results using vacuum treatment of the polymer solutions.<sup>51</sup> Water solution of lithium salt doped PEO was pumped in a closed chamber. As the result, statistical distribution of the 3D organized fibers has been fabricated. An optical microscopic image of such structures is shown in Figure 20(a). As the next step,

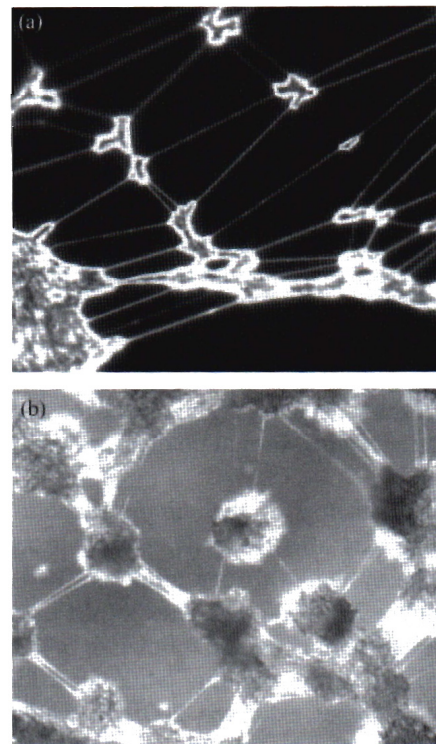


**Fig. 20.** Optical microscopy images of PEO (a) and PEO-PANI (b) fibrillar networks (image sizes are 0.6 × 0.5 mm). Reprinted with permission from [51], V. Erokhin et al., *Soft Matter* 2, 870 (2006). © 2006, The Royal Society of Chemistry.

this fibrillar structure was covered with PANI and pumped again. Such treatment resulted in the formation of the statistical 3D structure including PEO and PANI fibers. The image of the resulting structure is shown in Figure 20(b). The main question was whether the network is complex enough that suitable PEO-PANI junctions, similar to that in the deterministic memristor structures, were statistically realized. In order to check this hypothesis, the structure shown in Figure 21 was fabricated.<sup>51</sup> Reference electrode was placed into the PEO solution before pumping. Electrical characterization of the formed structure was performed similarly to the procedure for a single deterministic memristor.

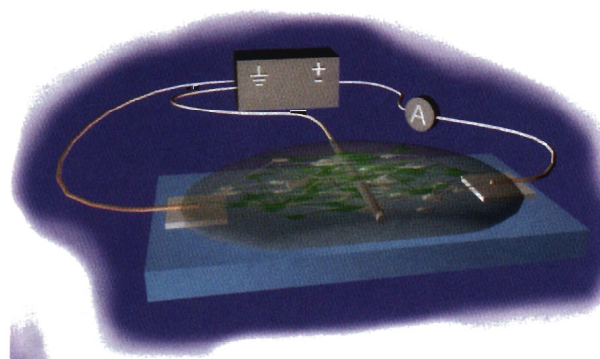


**Fig. 21.** Organic memristor based on statistical fiber structure.

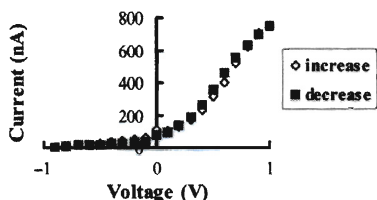


**Fig. 22.**  $V$ - $I$  characteristics measured on the drain electrode in a 3 electrode circuit. Reprinted with permission from [51], V. Erokhin et al., *Soft Matter* 2, 870 (2006). © 2006, The Royal Society of Chemistry.

Cyclic  $V$ - $I$  characteristics of the structure are shown in Figure 22. Pronounced rectifying behavior indicates the success in the statistical formation of zones with memristor properties.

A statistical analog of the circuit capable of supervised learning was also realized on fiber structures. The scheme of the system with one input and two outputs is shown in Figure 23, while the values of the output signals before and after training are the following: both output values were 20 nA before training, while after the training, the reinforced output exhibited 200 nA, while the other one remained at 20 nA. Reinforcement was obtained by the application of +1.2 V, while testing was measured applying +0.5 V.

Similarly to the network of deterministic elements, the statistical system has demonstrated the capability of supervised learning. However, the stability of properties was found to be very low. After 2 hours of working, the conductivity of the network had practically vanished. Therefore, for the application of the approach to the fabrication of working networks, it is necessary to stabilize its structure and properties.

Initial work in this direction is connected to the utilization of some rigid “skeletons” that must stabilize the network structure. Currently, we are using porous materials and glass fibers.

A typical SEM image of a statistical structure on fibrillar support is shown in Figure 24.

In the case of porous materials, the fibrillar networks were significantly stabilized, maintaining their structure

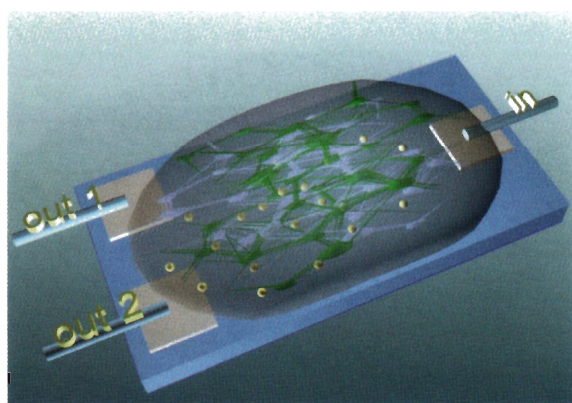


**Fig. 23.** Scheme of the adaptive network based on fibrillar structure.

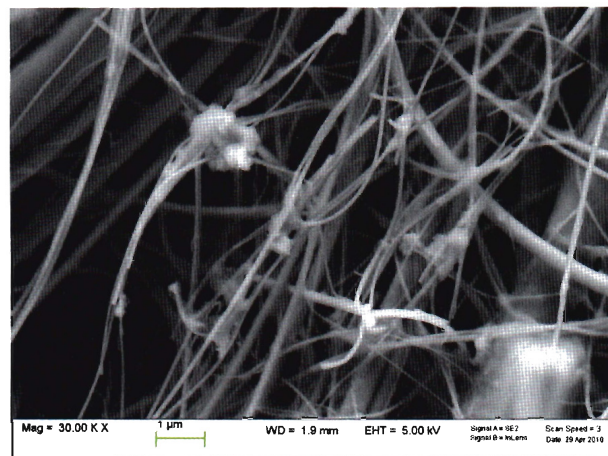


**Fig. 24.** SEM image of the fibrillar network organized on porous support.

even in the high vacuum conditions. The fibre diameters were within tens of nm range.

In the case of glass fibers, the approach was different. Initially, the fibers were covered with PANI and then the structure was used for the PEO fibers formation.<sup>46</sup>

## 8. CONCLUSIONS

In this review we have presented the results on the structure and properties of organic memristor—a material electrical element, combining properties of the resistor and memory, that can imitate the synaptic plasticity properties of biosystems.

Essential requirement to the memristor construction is the nm-range thickness of the conducting polymer channel—active area of the memristor. Lateral sizes of the device are currently in the millimeter to micron scale. However, there is no fundamental impediment to bringing them to the nano range by two approaches: application of the high resolution lithography and new bottom-up self-assembling and microphase separation processes, including the formation of statistically formed fibrillar networks. In addition, functionalized gold nanoparticles can be dispersed or connected into such structures, which would yield additional new electrical properties due to the Schottky effect and single-electron phenomena.<sup>52,53</sup>

Circuits, based on the memristors, have demonstrated the capabilities for adaptations, making them promising key components for new computer architectures, where these elements will serve for memory and processing functions simultaneously, yielding learning and information processing characteristics similar to those of biological cognitive systems.

Further development of this work can have fundamental and applied significance. From the basic point of view, the success in mimicking processes in nervous system will help to understand better processes occurring in the brain. Synthetic reconstruction of the nervous system fragments,

responsible for specific function execution, will support or refute the validity of the relative neuromodeling and simulations. As an example, we can refer to the work, soon to be published, where a reproduction of the part of the nervous system of the pond snail, responsible for the learning during feeding of the animal, has been realized. The model describing the learning of snail involves a heterosynaptic junction, based on two synapses, working in a cascade configuration. Thus, the mimicking circuit was based on two organic memristors and the results have confirmed the validity of the developed model.

From the applied point of view, namely, the realization of new computing systems, there are still a lot of questions to be answered. First, if the clock generator of the system which provides synchronization, is based on the oscillating element described in Section 5, the rhythm of the occurring processes can be variable depending on several parameters, such as environmental changes, history of the system functioning, aging etc. Obvious solution of the mentioned problem will demand the concentration of the efforts on the stabilization of the oscillating element properties. However, for the realization of a brain-like system, this solution is not so obvious anymore. In fact, the brain does not work in a constant mode and can be affected by a lot of external and internal factors. Is it an essential feature for learning and decision making? If so, we do not need to stabilize the clock generator properties allowing to the system to vary its rhythmic behavior.

The other applied problem is connected with the functioning of the system composed from a very large number of memristors. Thus, significant attention is paid now to model the behavior of complex deterministic and statistical networks with numerous elements.

After the successful material realization it will be necessary to make comparison of the synthetic system features with those of the brain. In particular, to perform a spacial-temporal mapping of the system domains properties during learning. This task will demand the development of special techniques, allowing to analyze the distribution of properties in a high-resolution non-destructive manner. Such work is currently in progress in our group and first encouraging results have been already obtained.

Finally, if the described approach will be completely successful, the important phenomena connected with order out of chaos could be addressed in a bio-inspired system: the complex adaptive network could show emergent behavior when random noise is used as input to the system.

**Acknowledgments:** We acknowledge the financial support of the Future and Emerging Technologies (FET) programme within the Seventh Framework Programme for Research of the European Commission, under the FET-OPEN grant agreement BION, number 213219.

## References

- D. O. Hebb, *The organization of behavior, A Neurophysiological Theory*, Second edn., Wiley and Sons, New York (1961).
- C. H. Bailey, M. Giustetto, Y.-Y. Huang, R. D. Hawkins, and E. R. Kandel, *Nat. Rev. Neurosci.* 1, 11 (2000).
- W. Zhang and D. J. Linden, *Nat. Rev. Neurosci.* 4, 885 (2003).
- P. R. Benjamin, G. Kemenes, and I. Kemenes, *Front. Biosci.* 13, 4051 (2008).
- V. Erokhin, A. Schüiz, and M. P. Fontana, *Int. J. Unconventional Computing* 6, 15 (2010).
- L. Chua, *IEEE Trans. Circuit Theory* 18, 507 (1971).
- D. B. Strukov, G. S. Snider, D. R. Stewart, and R. S. Williams, *Nature* 453, 80 (2008).
- J. J. Yang, M. D. Pickett, X. Li, D. A. A. Ohlberg, D. S. Stewart, and R. S. Williams, *Nat. Nanotechnol.* 3, 429 (2008).
- J. Borghetti, G. S. Snider, P. J. Kuekes, J. J. Yang, D. R. Stewart, and R. S. Williams, *Nature* 464, 873 (2010).
- J. Wu and R. L. McCreery, *J. Electrochem. Soc.* 156, 29 (2009).
- X. Cao, X. Li, X. Gao, W. Yu, X. Liu, Y. Zhang, L. Chen, and X. Cheng, *J. Appl. Phys.* 106, 073723 (2009).
- T. Driscoll, H.-T. Kim, B.-G. Chae, M. Di ventra, and D. N. Basov, *Appl. Phys. Lett.* 95, 043503 (2009).
- T. H. Kim, E. Y. Jang, N. J. Lee, D. J. Choi, K.-J. Lee, J. Jang, J. Choi, S. H. Moon, and J. Cheon, *Nano Lett.* 9, 2229 (2009).
- S. H. Jo, K.-H. Kim, and W. Lu, *Nano Lett.* 9, 496 (2009).
- L. A. Agapito, S. Alkis, J. L. Krause, and H.-P. Cheng, *J. Phys. Chem. C* 113, 20713 (2009).
- Y. V. Pershin and M. Di Ventra, *Phys. Rev. B* 78, 113309 (2008).
- J. Borghetti, Z. Li, J. Strazicky, X. Li, D. A. A. Ohlberg, W. Wu, D. R. Stewart, and R. S. Williams, *Proc. Natl. Acad. Sci. USA* 106, 1699 (2009).
- Q. Xia, W. Robinett, M. W. Cumbie, N. Banerjee, T. J. Cardinali, J. J. Yang, W. Wu, X. Li, W. M. Tong, D. B. Strukov, G. S. Snider, G. Medeiros-Ribeiro, and R. S. Williams, *Nano Lett.* 9, 3640 (2009).
- C.-F. Shu and M. S. Wrighton, *J. Phys. Chem.* 92, 5221 (1988).
- G. Bidan, *Sens. Actuators, B* 6, 45 (1992).
- T. Yamamoto, K. Sugiyama, T. Kushida, T. Inoue, and T. Kanbara, *J. Am. Chem. Soc.* 118, 3930 (1996).
- D. M. deLeeuw, M. M. J. Simenon, A. R. Brown, and R. E. F. Einerhand, *Synth. Met.* 87, 53 (1997).
- M. Chen, D. Nilsson, T. Kugler, M. Berggren, and T. Remonen, *Appl. Phys. Lett.* 81, 2011 (2002).
- M. Berggren and A. Richter-Dahlfors, *Adv. Mater.* 19, 3201 (2007).
- E. Said, P. Andersson, I. Engquist, X. Crispin, and M. Berggren, *Org. Electron.* 10, 1195 (2009).
- D. Nilsson, N. Robinson, M. Berggren, and R. Forchheimer, *Adv. Mater.* 17, 353 (2005).
- V. Erokhin, T. Berzina, and M. P. Fontana, *J. Appl. Phys.* 97, 064501 (2005).
- T. Berzina, A. Smerieri, M. Bernabo, A. Pucci, G. Ruggeri, V. Erokhin, and M. P. Fontana, *J. Appl. Phys.* 105, 124515 (2009).
- E. T. Kang, K. G. Neoh, and K. L. Tan, *Progr. Polym. Sci.* 23, 277 (1998).
- W. Lu, E. Smela, P. Adams, G. Zuccarello, and B. R. Matthes, *Chem. Mater.* 16, 1615 (2004).
- T. Berzina, A. Smerieri, G. Ruggeri, M. Bernabo, V. Erokhin, and M. P. Fontana, *Mater. Sci. Eng., C* 30, 407 (2010).
- V. Erokhin, G. Raviele, J. Glatz-Reichenbach, R. Narizzano, S. Stagni, and C. Nicolini, *Mater. Sci. Eng., C* 22, 381 (2002).
- G. B. Appetecchi, F. Alessandrini, M. Carewska, T. Caruso, P. P. Prosini, S. Scaccia, and S. Passerini, *J. Power Sources* 97–98, 790 (2001).
- T. Berzina, V. Erokhin, and M. P. Fontana, *J. Appl. Phys.* 101, 024501 (2007).

35. S. Stafstrom, J. L. Bredas, A. J. Epstein, H. S. Woo, D. B. Tanner, W. S. Huang, and A. G. MacDiarmid, *Phys. Rev. Lett.* 59, 1464 (1987).
36. V. Erokhin, Polymer-based adaptive networks, *The New Frontiers of Organic and Composite Nanotechnologies*, edited by V. Erokhin, M. K. Ram, and O. Yvuz, Elsevier, Oxford (2007), pp. 287–353.
37. T. Berzina, S. Erokhina, P. Camorani, O. Konovalov, V. Erokhin, and M. P. Fontana, *ACS Appl. Mater. Interfaces* 1, 2115 (2009).
38. W. B. Yun and J. M. Bloch, *J. Appl. Phys.* 68, 1421 (1990).
39. K. Rossberg, G. Paasch, L. Dunsch, and S. Ludowig, *J. Electroanal. Chem.* 443, 49 (1998).
40. A. Smerieri, V. Erokhin, and M. P. Fontana, *J. Appl. Phys.* 103, 094517 (2008).
41. A. N. Zaikin and A. M. Zhabotinsky, *Nature* 225, 535 (1970).
42. R. Toth, C. Stone, A. Adamatzky, B. D. Costello, and L. Bull, *J. Chem. Phys.* 129, 184708 (2008).
43. V. Erokhin, T. Berzina, P. Camorani, and M. P. Fontana, *J. Phys. Condens. Matter* 19, 205111 (2007).
44. P. R. Benjamin, K. Staras, and G. Kemenes, *Learning and Memory* 7, 124 (2000).
45. A. Smerieri, T. Berzina, V. Erokhin, and M. P. Fontana, *Mater. Sci. Eng., C* 28, 18 (2008).
46. A. Smerieri, T. Berzina, V. Erokhin, and M. P. Fontana, *J. Appl. Phys.* 104, 114513 (2008).
47. V. Erokhin, T. Berzina, and M. P. Fontana, *Cryst. Rep.* 52, 159 (2007).
48. V. Erokhin, T. Berzina, P. Camorani, and M. P. Fontana, *Colloids Surf., A* 321, 218 (2008).
49. V. Erokhin, T. Berzina, S. Erokhina, and M. P. Fontana, *Organic memristor and adaptive networks, Nano-Net*, edited by A. Schmid, S. Goel, W. Wang, V. Beiu, and S. Carrara, Springer, Berlin (2009), pp. 210–221.
50. I. D. Norris, M. M. Shaker, F. K. Ko, and A. G. MacDiarmid, *Synth. Met.* 114, 109 (2000).
51. V. Erokhin, T. Berzina, P. Camorani, and M. P. Fontana, *Soft Matter* 2, 870 (2006).
52. V. Erokhin, P. Facci, S. Carrara, and C. Nicolini, *J. Phys. D: Appl. Phys.* 28, 2534 (1995).
53. V. Erokhin, P. Facci, S. Carrara, and C. Nicolini, *Thin Solid Films* 284–285, 891 (1996).

Received: 18 February 2010. Accepted: 12 May 2010.